

Article

# The Origin of Hydrocarbon Gases in the Lovozero Nepheline-Syenite Massif (Kola Peninsula, NW Russia), as Revealed from He and Ar Isotope Evidence

Valentin Nivin 

Geological Institute, Kola Science Centre, Russian Academy of Sciences, 14 Fersman St., 184209 Apatity, Russia; nivin@geoksc.apatity.ru; Tel.: +7-815-55-79-580

Received: 15 August 2020; Accepted: 16 September 2020; Published: 21 September 2020



**Abstract:** The occurrence of hydrocarbon gases (HCG) in unusually high concentrations for magmatic complexes, in the Lovozero and some other alkaline massifs, is of both geochemical and practical interest. The nature of these gases, despite the long history of research, remains the subject of debate. As an approach to solving this problem, we studied the coupled distribution of occluded HCG and the recognized tracers of various geological processes, such as helium and argon isotopes. The extraction of the gas components trapped in fluid micro-inclusions was carried out by the mechanical crushing of rock and mineral samples. A positive correlation was found between the  $^3\text{He}/^4\text{He}$  and  $\text{CH}_4/\text{C}_2\text{H}_6$  ratios, whereas a negative correlation of the latter was found with the  $^{36}\text{Ar}$  concentration, which in turn was directly related, in varying degrees, to the content of HCG and most strongly with pentanes. Conjugacy of the processes of the heavier gaseous hydrocarbons, a loss of the deep component of the fluid phase and dilution of it with the atmogenic component was established. In the absence of a correlation between  $\text{CH}_4$  and  $^3\text{He}$ , the value of the  $\text{CH}_4/{}^3\text{He}$  ratio in the Lovozero gas substantially exceeded the estimates of it in gases of a mantle origin, and mainly corresponded to the crustal values. However, in some samples, a small fraction of mantle methane was allowed. The peculiarities of the relationships between hydrocarbon gases and the isotopes of noble gases indicate a sequential process of abiogenic generation and transformation of HCG at the magmatic and post-magmatic stages during the formation of the Lovozero massif. The obtained results confirm the usefulness of this approach in solving the origin of reduced gases in alkaline igneous systems.

**Keywords:** abiogenic hydrocarbon gases; methane; He and Ar isotopes; nepheline syenite; fluid inclusions; magmatic complexes

## 1. Introduction

A notable feature of some nepheline syenite and foidolite massifs, primarily in the world's largest Khibiny and Lovozero alkaline plutons and the related huge deposits of phosphorus and rare elements, as well as in Ilimaussaq in Greenland, is a concentration of reduced hydrogen-hydrocarbon that is unusually high for igneous rocks, with a predominance of methane gases [1–6]. Commonly, hydrocarbon gases (HCG) are found in vacuoles of micro-inclusions in minerals (occluded gases—OG). Still, the occurrence of other forms (morphological types) of such gases are also known in the Khibiny and Lovozero massifs. These freely released, or free gases (FG), are filling systems with varying degrees of interconnected fractures (mainly microfractures), as well as other cavities in the rocks, and diffusely dispersed gases (DDG) that are found in closed and half-open thin and sub-capillary cracks, retained, to a considerable extent, in the adsorbed state, and where diffusion transfer predominates when they are moving [1,4,6–9].

The presence and nature of HCG in the rocks of agpaitic complexes is of both geochemical and practical interest. In particular, the first matter is due to the importance of clarifying the role of reduced fluids as possible agents and indicators of the conditions and sequence of the rock and mineral formation, including various types of ore mineralization (e.g., References [5,10–17]). The applied value is due to the release of hazardous natural combustible and explosive gases into the atmosphere of the underground mines working on mineral deposits associated with nepheline-syenite massifs [1,4,6,9]. The solution to these and other problems is impossible without learning more about the origin of these gases.

However, despite more than half a century history of studies focused on HCG in the rocks of these massifs, the mechanisms and the relative time of their formation are still subject to discussion [6,7,11–15,17–25]. With a wide range of assumptions being made about the genesis of HCG (from biogenic to mantle origins), most researchers consider these gases to be abiogenic. To explain the pre-, early-, late-, or post-magmatic formation of these gases, various authors have considered all the processes and mechanisms of abiogenic methane formation, such as, in Etiope and Sherwood Lollar [26], Sephton and Hazen [27]. Different directions of the evolution of the hydrocarbons—from complex compounds to the simplest and vice versa—have also been assumed.

The various points of view on the nature of HCG (in most cases, OG are referred to) proposed by the authors, especially in recent publications, have been based on data concerning the features of their distribution in rocks and minerals, the isotopic composition of the carbon and hydrogen, thermodynamic calculations and the thermometry of individual fluid inclusions. Meanwhile, rare gas isotopes have long been used and are increasingly recognized as geochemical tracers for various processes in the fluid and fluid-containing systems of different geological environments [28–50]. In our case, we used an approach that was not previously employed to understand some aspects of the origin of the reduced fluid in nepheline-syenite magmatic complexes, as well as for studying the coupled distribution of occluded HCG and helium and argon isotopes in the rocks of the Lovozero massif. The results of these studies are presented in this article.

## 2. Geological and Gas Geochemical Settings

### 2.1. Lovozero Massif

The Lovozero massif of agpaitic feldspathoid (mainly nepheline) syenites and foidolites has been the subject of detailed and comprehensive studies. Research results on various aspects of its geology, petrology, mineralogy, geochemistry and metallogeny are revealed in hundreds of publications, including monographs (e.g., References [51–54]) and relatively recent articles [55–63]. The presence of such an extensive range of literature has allowed us to confine the scope of the current research to only the most general information on the geology of the massif, sufficient for understanding the subject of the article. For some rocks, the names that are not generally accepted, but are the most commonly used, have been preserved.

According to the totality of the available data, the laccolith-type Lovozero alkaline massif was emplaced 360–370 million years ago into Archean gneisses and gneiss-diorites covered by Devonian sedimentary-volcanogenic rocks, at the peak of the Palaeozoic tectono-magmatic activation of the eastern part of the Fennoscandian shield. The rocks of the differentiated complex (DC, also known as layered and loparite-bearing) and the eudialyte complex (EC), are predominant within the recent erosional truncation (Figure 1). The names of these complexes are somewhat arbitrary.

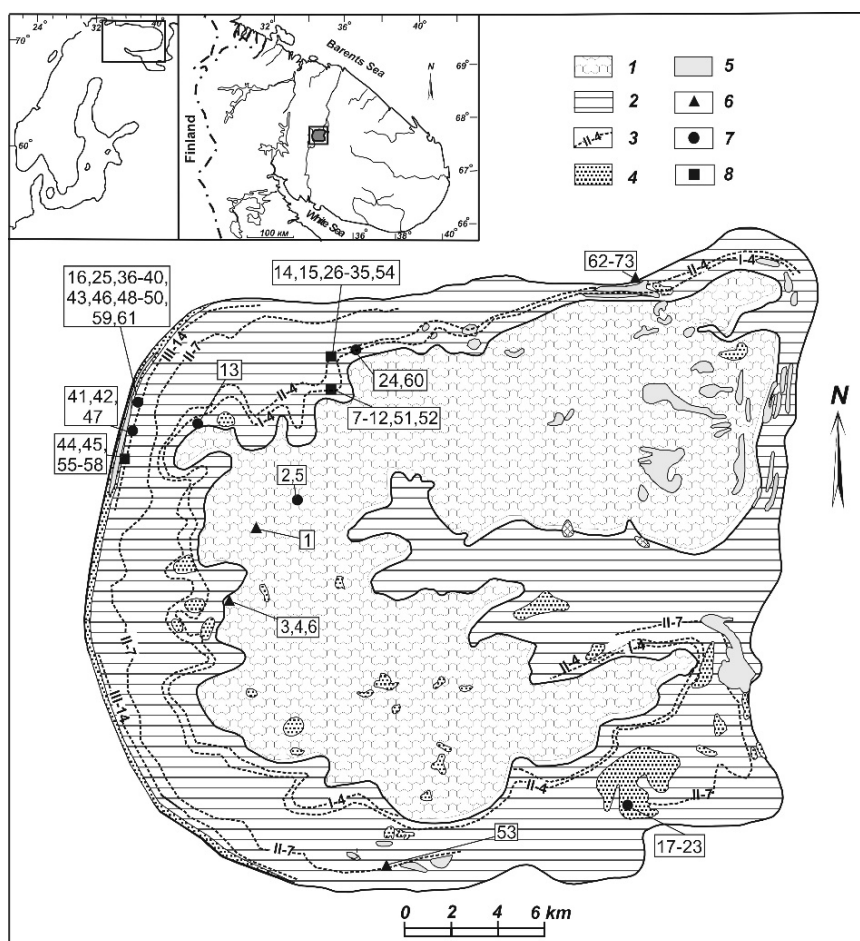


**Figure 1.** Geological sketch-map of the Lovozero massif (based on the map of PGO Sevzapgeologiya). 1 and 2—rocks of the eudialyte and differentiated complexes, respectively; 3—marker ore horizons; 4—poikilitic and inequigranular feldspathoid syenites; 5—remnants of the sedimentary-volcanogenic series; sampling sites (the sample numbers correspond to those in Table 1): 6—natural outcrops; 7—boreholes; 8—underground mine workings.

**Table 1.** Brief sample characteristics.

Sample Number	Rock <sup>1</sup> /Mineral	Geological Position <sup>2</sup>
1	Eudialyte feldspar urtite with loparite	EC
2	Eudialyte foyaite	EC
3	Eudialyte lujavrite	EC
4	Eudialyte lujavrite	EC
5	Eudialyte lujavrite	EC
6	Murmanite-eudyalite lujavrite	EC
7	Feldspar urtite	DC, I-1
8	Loparite urtite	DC, I-4
9	Zeolitized feldspar urtite	DC, I-4
10	Nepheline from feldspar urtite	DC, I-4
11	Feldspar from urtite	DC, I-4
12	Sodalite from feldspar urtite	DC, I-4
13	Feldspar urtite	DC, series I
14	Zeolitized urtite	DC, II-4
15	Loparite malignite	DC, II-4
16	Zeolitized urtite	DC, II-5
17	Urtite	DC, III-1

Table 1. Cont.

Sample Number	Rock <sup>1</sup> /Mineral	Geological Position <sup>2</sup>
18	Feldspar urtite	DC, series IV
19	Ijolite-urtite	DC, series V
20	Trachytoid feldspar urtite	DC, series V
21	Trachytoid feldspar urtite	DC, series V
22	Trachytoid feldspar urtite	DC, series V
23	Nepheline from feldspar urtite	DC, series V
24	Zeolitized foyaite	DC, above I-2
25	Foyaite	DC, II-1
26	Foyaite with villiaumite and eudialite	DC, II-3
27	Analcime-bearing foyaite	DC, II-4
28	Albitized foyaite	DC, II-4
29	Zeolitized foyaite	DC, below II-4
30	Foyaite	DC, below II-4
31	Foyaite with sodalite and cancrinite	DC, below II-4
32	Nepheline from foyaite	DC, below II-4
33	Feldspar from foyaite	DC, below II-4
34	Clinopyroxene from foyaite	DC, below II-4
35	Sodalite from foyaite	DC, below II-4
36	Eudialite-bearing foyaite	DC, above II-5
37	Eudialite-bearing foyaite	DC, above II-5
38	Eudialite-bearing foyaite	DC, above II-5
39	Foyaite	DC, below II-5
40	Foyaite	DC, above II-7
41	Apatite- and eudialite-bearing foyaite	DC, above III-1
42	Foyaite with eudialite	DC, above III-1
43	Foyaite	DC, above III-8
44	Villiaumite-bearing foyaite	DC, III-14
45	Villiaumite-bearing foyaite	DC, III-14e
46	Foyaite	DC, above III-15
47	Eudialite-bearing foyaite	DC, below III-16
48	Eudialite-bearing foyaite	DC, below III-16
49	Foyaite	DC, above IV-1
50	Foyaite	DC, below IV-5
51	Foyaite	DC, below IV-5
52	Zeolitized lujavrite	DC, I-4
53	Zeolitized loparite lujavrite	DC, I-4
54	Lujavrite with amphibole	DC, II-7
55	Amphibole lujavrite	DC, series II
56	Lujavrite	DC, III-14
57	Lujavrite	DC, III-14
58	Loparite lujavrite with villiaumite	DC, III-14
59	Loparite lujavrite	DC, III-14
60	Poikilitic nepheline syenite	DC, below III-2
61	Poikilitic nepheline syenite	DC, above III-14
62	Coarse-grained nepheline syenite	ENCM
63	Coarse-grained nepheline syenite	ENCM
64	Coarse-grained nepheline syenite	ENCM
65	Pegmatoid nepheline syenite	ENCM
66	Pegmatoid nepheline syenite	ENCM
67	Pyroxene-feldspar fenite	EXCM
68	Pyroxene-feldspar fenite	EXCM
69	Fenitized gneiss	EXCM
70	Fenitized gneiss	EXCM
71	Fenitized gneiss	EXCM
72	Fenitized gneiss	EXCM
73	Biotite gneiss	EXCM

<sup>1</sup> If other characteristics are not given, the rock is mesocratic medium-grained massive (all lujavrites are trachytoid).

<sup>2</sup> DC is the differentiated complex (I-1–III-16 is the number of the series plus the number of the horizon (layer), EC is the eudialite complex, ENCM and EXCM are the endocontact and exocontact of the massif.

The DC, where the ore (loparite) bodies are mainly concentrated, is composed of numerous (up to 200) gently pitching, rhythmically alternating horizons (layers) of lujavrites (trachitoid nepheline syenites of the foyaite-malignite-shonkinite series), as well as massive foyaites and urtites forming two-member and three-member sequences. The thickness of the individual layers varies from several centimeters to dozens of meters. The DC is usually divided into series (I–V from top to bottom) consisting of several (up to 16) rhythms. For the marker foidolite horizons, including the ore-bearing ones, a nomenclature that involves a serial and order number of the horizon from the upper border of the series (for example, I-4, II-7, III-14, etc.) is acceptable. In addition to the above-mentioned rocks, the differentiated complex also includes alkaline rock varieties, such as ijolite and malignite. The main rock-forming minerals are nepheline, K-Na feldspar and aegirine. The ore mineral of loparite, or more exactly, loparite-(Ce) with the general formula  $(\text{Na,Ce,Ca})_2(\text{Ti,Nb})_2\text{O}_6$ , occurs in sheet-like zones and ledges of dissemination related mostly to areas of contact between rocks of different petrographical compositions. Near the contact of the massif, the DC rocks are gradually being replaced by massive coarse-grained and pegmatoid nepheline syenites. The gneisses in the exocontact intrusion are fenitized to varying degrees. The fenites themselves form narrow zones, ranging from fractions of a meter to several meters.

The EC is generally made up of a slightly differentiated stratum of inequigranular eudialyte lujavrites (eudialyte malignites), locally changing into foyaites, and rarely into foidolites. The rocks are enriched with (mangano) eudialyte in amounts of 5 to 10 vol.%, while sometimes reaching 90 vol.%.

Both complexes contain numerous bodies of poikilitic and inequigranular nepheline, sodalite-nepheline and nosean-nepheline syenites, concordant lens-like or sheet-like xenoliths of olivine basalts, tuffs and tuffites of the Lovozero Suite, as well as alkaline pegmatites and hydrothermalites, in various sizes and shapes.

## 2.2. Occluded Hydrocarbon Gases

As in other morphological types of the gas phase in the Lovozero massif [6,8,9], methane is the main component of the gases occluded in vacuoles of fluid inclusions in the minerals [1,4,6,25,64,65]. Most often, these inclusions are gaseous and secondary in the relative formation time. When a gas extraction is carried out by mechanical grinding of the samples, the  $\text{CH}_4$  concentration in OG according to a chromatographic analysis is mainly 70–90 vol.%. In varying subordinate and trace amounts, hydrogen, ethane, other methane homologues (up to pentanes inclusive), unsaturated HCG (alkenes), nitrogen and helium are always present. Dioxide, and especially carbon monoxide, are occasionally detected and, as a rule, exist only in low concentrations. The specific content of  $\text{CH}_4$  in the rocks and minerals on average (median) values of 6–8  $\text{cm}^3/\text{kg}$  can reach 100  $\text{cm}^3/\text{kg}$ . With a decrease in this characteristic, the relative concentration of non-hydrocarbon components in the exhaust gas increases.

The most important gas concentrating minerals are nepheline and K-Na feldspar [14,66]. Of the three main types of rocks, lujavrites are generally less gas-saturated than foyaites and urtites. However, the HCG content level is more dependent on the position of the sample in a vertical section of the massif, not on the petrographic type of the rock. So, in the differentiated complex, the same rocks gas saturation is significantly higher in the III–V series compared to the I and II series [4,15,22]. The content of HCG in EC rocks is comparable with that of the upper part of the DC. A positive correlation has been found between the gas saturation of the Lovozero rocks and the content of late- and post-magmatic sodalite, analcime, albite and villiaumite in these rocks, as well as a negative correlation between the contents of the gases and low-temperature zeolites of the natrolite group [4,15]. An important indicator role was also established for the  $\text{CH}_4/\text{C}_2\text{H}_6$  ratio ( $R_{\text{ME}}$ ), where a decrease in this ratio, as well as an increase in the slope of the HCG molecular weight distribution corresponding to the classic Anderson–Schulz–Flory distribution, reflects a decrease in the temperature range of the post-magmatic processes, gas generation and the capture of fluid inclusions [14,15,22,23,66].

As was already noted, the mechanisms, conditions and relative time for the formation of HCG in the rocks of the Khibiny, Lovozero and Ilmaussaq nepheline-syenite massifs have been the subject of

discussion for an extended period of time. Reviews of the hypotheses concerning their origin (from biogenic to mantle origins) contain varying degrees of detail; for example, in References [4,6,15,22,67]. Nonetheless, the vast majority of modern researchers, with rare exceptions (e.g., Reference [24]), consider these gases to be predominantly abiogenic, and one way or another related to the formation of the massifs.

### 2.3. He and Ar Isotope Compositions

The data on the isotopic composition of helium and argon in the rocks and minerals of the Lovozero massif was partially published earlier [68,69], and is systematized and generalized in Reference [70]. Compared with the other Palaeozoic complexes of the Kola alkaline province, especially alkaline ultrabasic with carbonatites in the mantle fluid of which the contribution of a  $^3\text{He}$ -rich plume component was established [71,72], the rocks of the Lovozero massif that are undoubtedly the mantle source of parental melts [73–75] have retained the primary mantle gases to the least extent, and on the contrary, are more susceptible to the influence of surface meteoric waters containing dissolved atmospheric air. They differ in terms of the lowest  $^3\text{He}/^4\text{He}$  and  $^{40}\text{Ar}/^{36}\text{Ar}$  ratios in the gases occluded in fluid inclusions. Thus, the estimated initial  $^3\text{He}/^4\text{He}$  ratio in the trapped fluid here was  $1.2 \times 10^{-6}$  [70], while in the Seblyavr and Kovdor alkaline-ultrabasic massifs with carbonatites, this ratio was  $\sim 3.3 \times 10^{-4}$  [72]. The Lovozero rocks and minerals are characterized by wide variations in the concentrations of helium isotopes ( $(0.45\text{--}960) \times 10^{-6}$  and  $(0.37\text{--}600) \times 10^{-13}$   $\text{cm}^3/\text{g}$  respectively,  $^4\text{He}$  and  $^3\text{He}$ ), as well as argon ( $(7.6\text{--}2200) \times 10^{-8}$  and  $(2.2\text{--}210) \times 10^{-10}$   $\text{cm}^3/\text{g}$  respectively,  $^{40}\text{Ar}$  and  $^{36}\text{Ar}$ ) and the indicator isotopic ratios  $^3\text{He}/^4\text{He}$  and  $^{40}\text{Ar}/^{36}\text{Ar}$  ( $(0.5\text{--}110) \times 10^{-8}$  and 311–5450, respectively) in the occluded gases [70]. It has been established that the  $^3\text{He}$  in OG is mainly mantle, while the  $^{36}\text{Ar}$  is predominantly atmogenic. The decrease in the  $^3\text{He}/^4\text{He}$  and  $^{40}\text{Ar}/^{36}\text{Ar}$  ratios generally reflects an increase in the degree of degassing in the primary fluid and/or adding to it the core, in particular, the atmogenic component. The variations in these indicators, as in the case of HCG, are caused to a great extent by the positions of the samples in the vertical section of the massif, and not by the petrographic type of rock.

In general, the features of the distribution of the isotopes of noble gases in the rocks and minerals of the Lovozero massif confirm: (a) the general direction of the evolution of the melt and the complementary fluid phase in the magma chamber as a whole, in the three-membered (urtite-foyaite-lujavrite) units and in each individual layer. (b) The relative closeness of the fluid-rock-melt system during the magmatic crystallization and in the early stages of the epimagmatic transformations, with a predominantly auto-metasomatic character. (c) A shorter time interval and a temperature gradient between the formation of a crystalline matrix and fluid inclusions in the ore rocks relative to the barren rocks. (d) The possibility of transforming the ore horizons at a relatively late post-magmatic stage and (e) the important role of paleometeor waters in the low-temperature mineralogenesis [70].

### 3. Samples and Analytical Methods

The distribution of He and Ar isotopes and the content of HCG were studied in the same rock samples. To a lesser extent, the minerals of the massif itself, as well as the zone of its contact with the gneisses, were included in the study (Table 1).

The extraction of the gas components contained in the fluid inclusions was carried out by the mechanical grinding of rock and mineral samples. Two modifications of this method were used for the extraction of HCG from large (200–350 g) and small (0.5–1 g) weights [4]. Crushing of the large samples was carried out for 20 min on a vibration eraser in special, sealed stainless-steel cups with grinding balls, which were previously vacuumized up to 1.3 Pa. When the fraction  $-10 + 1$  mm was loaded into the beaker, about 60–70% of the sample was crushed to 0.05 mm particles. After grinding the sample, the evolved gas was pumped out via a mercury unit and was then introduced into the chromatograph PE F-30 (PerkinElmer Inc., UpplandsVäsby, Sweden) and TSVET-102 (LLC “Tsvet”, Dzerzhinsk, Russia), using a syringe. In the second case, a small (about  $2.5 \text{ cm}^3$ ) volume

vibrochamber built into the gas system of the TSVET-102 chromatograph was used, into which the sample fraction of  $-0.63 + 0.25$  mm was loaded together with the grinding balls and purged with helium. The grinding was carried out for 20 min in a helium atmosphere at room temperature and pressure. After switching the metering valve, the evolved gases were washed out by the carrier gas into the chromatographic column. The minimum detectable concentrations of the individual gases varied somewhat, depending on the type of chromatograph and the sorbent that was used. They averaged (as a percentage by volume) 0.0005, 0.00005 and 0.00001 for methane, ethane and the heavier HCG, respectively. The root-mean-square error of the analysis of individual components was 0.4–0.8, while the coefficient of variation ranged from 2.7% to 4.6%.

The methodology used to study the isotopic composition of helium and argon has been repeatedly published in earlier research, for example in References [70–72] (and references therein). The extraction of the occluded noble gases was carried out by a mechanical grinding of the samples. A 0.25–0.6 mm fraction of a sample weighing 1.5–2 g was placed in a glass ampoule together with the grinding steel rollers and/or balls and was then evacuated and soldered. The grinding was carried out on a vibration unit. Titanium-zirconium getters absorbed the chemically active components of the released gases. Separation of the light and heavy noble gases was carried out using coal traps cooled by liquid nitrogen. The contents and isotopic composition of helium and argon were measured on a MI-1201 static mass spectrometer. The sensitivity for helium and argon is  $5 \times 10^{-5}$  and  $3 \times 10^{-4}$  A/torr, respectively. The error in determining the concentrations (determined using the peak height method) was 5% ( $\pm 1 \sigma$ ). The  $^3\text{He}/^4\text{He}$  ratios at values of  $10^{-6}$  and  $10^{-8}$  were measured with errors of  $\pm 2\%$  and  $\pm 20\%$ , respectively. The measurement error of the  $^{40}\text{Ar}/^{36}\text{Ar}$  ratio of 3000 was 0.3%, while for a value of 50,000, the error was 25%. The volume of the gas was reduced to normal conditions. The measurements were performed by I. L. Kamensky and under his methodical guidance by the author.

#### 4. Results and Discussion

When the distribution of the isotopes of noble gases was separately studied in earlier research, as well as methane and its homologues in Lovozero rocks, attention was drawn to the similar peculiar properties of the variations in the vertical section of the massif in the average  $^3\text{He}/^4\text{He}$  and  $\text{CH}_4/\text{C}_2\text{H}_6$  ratios [22,23,70]. As was noted above (Sections 2.2 and 2.3), a decrease in the first of these indicator ratios indicates a loss in the fluids of the primary mantle component [70,72]. In contrast, the second ratio reflects a decrease in the temperature range of the HCG generation, post-magmatic changes in the minerals and the formation of fluid inclusions [14,23,66,70]. In each of the three main types of Lovozero rocks (lujavrite, foyaite and urtite), from the top to the bottom of the section, both of these indicators slightly increased from the eudialyte complex to the first series of DC, followed by a significant decrease in the lower zone of the first and upper parts of the second series, reaching its minimum in the ore (loparite) ledges, then gradually and significantly increased with a greater depth. In the same direction (from top to bottom), the  $^{40}\text{Ar}/^{36}\text{Ar}$  ratio increased and the  $^{36}\text{Ar}$  concentration decreased more smoothly. The most likely and main source of the latter phenomenon was paleometeor water with air dissolved [70]. The peculiarity of the change in  $R_{\text{ME}}$  is consistent with the molecular mass distribution of heavier gaseous alkanes in both rocks and minerals [14,23].

Additional studies and a direct comparison of the gas-geochemical characteristics of the same samples confirmed these presumed relationships. Table 2 presents the results of measurements in the rocks and minerals of the concentrations, with the ratios of the isotopes of noble gases and the content of hydrocarbon gases. The concentrations of  $^4\text{He}$ ,  $\text{CH}_4$ ,  $\text{C}_2\text{H}_6$  and the ratio  $^3\text{He}/^4\text{He}$  were determined in almost all the samples, while the isotopic composition of argon and the content of pentanes were determined in less than half of them. Variations in most of these parameters, with the exception of  $^{40}\text{Ar}$  and  $^{40}\text{Ar}/^{36}\text{Ar}$ , reached three orders of magnitude.

Table 2. He and Ar isotope abundances and concentrations of hydrocarbon gases.

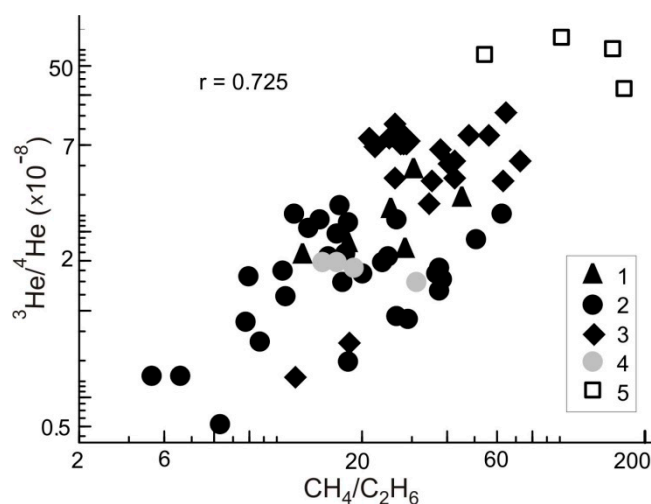
Sample <sup>1</sup>	<sup>4</sup> He 10 <sup>-6</sup> cm <sup>3</sup> /g	<sup>3</sup> He/ <sup>4</sup> He 10 <sup>-8</sup>	<sup>40</sup> Ar 10 <sup>-6</sup> cm <sup>3</sup> /g	<sup>40</sup> Ar/ <sup>36</sup> Ar	CH <sub>4</sub> 10 <sup>-3</sup> cm <sup>3</sup> /g	C <sub>2</sub> H <sub>6</sub> 10 <sup>-4</sup> cm <sup>3</sup> /g	∑C <sub>5</sub> H <sub>12</sub> <sup>2</sup> 10 <sup>-7</sup> cm <sup>3</sup> /g
1	0.9	12.0	2.5	524	11.5	2.5	n.a. <sup>3</sup>
2	0.8	10.2	3.4	378	5.0	2.0	n.a.
3	0.6	17.5	3.3	603	20.7	6.8	43.0
4	2.4	6.4	n.a.	n.a.	2.5	1.4	6.4
5	3.3	5.8	1.5	496	4.6	1.6	n.a.
6	1.8	5.5	n.a.	n.a.	1.4	1.1	n.a.
7	2.1	4.2	n.a.	n.a.	16.8	4.5	n.a.
8	190	1.0	n.a.	n.a.	2.2	6.0	n.a.
9	260	7.2	n.a.	n.a.	31.2	18.9	n.a.
10	71.0	7.7	4.5	573	27.8	21.3	63.0
11	20.3	8.5	4.1	513	31.2	17.5	38.9
12	33.0	8.8	7.8	362	56.3	39.4	137
13	2.3	2.2	1.2	590	23.0	7.9	n.a.
14	47.0	3.0	n.a.	n.a.	9.8	9.1	n.a.
15	632	1.0	n.a.	n.a.	2.7	5.8	n.a.
16	2.4	4.0	n.a.	n.a.	7.7	9.5	n.a.
17	36.1	34.0	4.9	944	3.7	1.4	n.a.
18	5.3	15.3	7.7	3446	35.8	10.1	n.a.
19	64.8	19.2	13.9	3602	41.0	10.0	n.a.
20	63.7	15.8	n.a.	n.a.	1.5	0.6	n.a.
21	329	16.0	n.a.	n.a.	16.3	3.8	7.3
22	295	20.0	2.2	491	16.3	3.8	7.3
23	297	20.2	5.6	2760	22.7	3.1	n.a.
24	1.2	4.9	3.5	394	17.7	7.4	n.a.
25	1.6	4.1	1.4	461	6.1	3.0	12.0
26	4.9	3.8	n.a.	n.a.	20.5	5.3	n.a.
27	37.0	4.5	n.a.	n.a.	13.0	3.4	n.a.
28	25.0	2.3	n.a.	n.a.	0.4	0.2	n.a.
29	47.0	1.2	n.a.	n.a.	26.3	14.6	n.a.
30	2.2	4.3	n.a.	n.a.	4.4	4.2	n.a.
31	21.9	5.2	n.a.	n.a.	47.2	18.7	n.a.
32	42.5	5.3	4.2	661	41.1	26.6	46.0
33	7.7	5.4	12.2	1141	72.4	41.1	72.0
34	9.6	10.8	1.0	400	1.8	1.1	n.a.
35	29.0	5.0	7.1	661	47.9	31.4	82.0
36	1.1	6.5	n.a.	n.a.	64.3	12.6	27.4
37	1.4	3.7	n.a.	n.a.	5.6	3.3	9.9
38	0.8	8.6	n.a.	n.a.	4.3	1.6	n.a.
39	0.8	9.6	2.9	481	5.3	4.6	n.a.
40	2.0	9.4	4.5	1115	0.7	0.1	n.a.
41	6.0	24.0	n.a.	n.a.	73.7	33.5	n.a.
42	7.7	26.8	n.a.	n.a.	86.6	39.7	360
43	20.7	28.3	4.2	1565	41.8	8.8	n.a.
44	25.5	26.0	6.2	1675	96.6	33.3	n.a.
45	6.8	25.2	2.7	792	46.8	16.7	n.a.
46	32.0	29.1	3.9	681	56.7	10.2	n.a.
47	32.0	25.0	n.a.	n.a.	87.7	30.6	n.a.
48	24.0	30.2	n.a.	n.a.	101	36.4	116
49	30.3	40.0	6.8	5449	0.7	0.1	n.a.
50	18.7	23.6	5.0	1524	55.7	14.8	n.a.
51	26.7	27.4	8.8	1432	46.8	18.7	n.a.
52	4.4	1.6	n.a.	n.a.	0.1	0.1	n.a.
53	145	0.5	n.a.	n.a.	0.5	0.8	n.a.
54	6.3	3.2	n.a.	n.a.	2.5	0.7	n.a.
55	14.4	2.1	n.a.	n.a.	2.3	2.9	n.a.
56	7.6	10.9	6.6	1579	19.3	5.6	n.a.

Table 2. Cont.

Sample <sup>1</sup>	<sup>4</sup> He 10 <sup>-6</sup> cm <sup>3</sup> /g	<sup>3</sup> He/ <sup>4</sup> He 10 <sup>-8</sup>	<sup>40</sup> Ar 10 <sup>-6</sup> cm <sup>3</sup> /g	<sup>40</sup> Ar/ <sup>36</sup> Ar	CH <sub>4</sub> 10 <sup>-3</sup> cm <sup>3</sup> /g	C <sub>2</sub> H <sub>6</sub> 10 <sup>-4</sup> cm <sup>3</sup> /g	∑C <sub>5</sub> H <sub>12</sub> <sup>2</sup> 10 <sup>-7</sup> cm <sup>3</sup> /g
57	13.0	15.0	6.1	1123	9.5	1.5	n.a.
58	49.5	1.6	5.0	1572	14.3	8.0	n.a.
59	70.0	1.0	3.9	1231	8.6	7.4	n.a.
60	57.5	25.9	6.2	2836	2.0	0.7	n.a.
61	27.0	27.0	n.a.	n.a.	1.1	0.5	n.a.
62	1.5	4.8	n.a.	n.a.	0.6	0.4	n.a.
63	6.0	4.8	n.a.	n.a.	6.0	4.1	n.a.
64	0.8	4.4	n.a.	n.a.	1.0	0.5	n.a.
65	n.a.	n.a.	n.a.	n.a.	0.9	0.4	n.a.
66	1.0	3.7	n.a.	n.a.	1.3	0.4	n.a.
67	0.5	85.0	n.a.	n.a.	2.9	0.5	1.3
68	0.5	110.7	n.a.	n.a.	4.5	0.4	n.a.
69	0.8	78.0	n.a.	n.a.	n.a.	n.a.	n.a.
70	7.0	93.0	n.a.	n.a.	7.0	0.5	n.a.
71	0.7	54.0	n.a.	n.a.	13.0	0.8	n.a.
72	n.a.	n.a.	n.a.	n.a.	5.3	0.3	n.a.
73	0.7	17.4	n.a.	n.a.	1.9	n.a.	n.a.

<sup>1</sup> The sample numbers correspond to those in Table 1. <sup>2</sup> iC<sub>5</sub>H<sub>12</sub> + nC<sub>5</sub>H<sub>12</sub>. <sup>3</sup> n.a.—not analyzed.

Between the ratios of CH<sub>4</sub>/C<sub>2</sub>H<sub>6</sub> and <sup>3</sup>He/<sup>4</sup>He, a generally positive correlation was found (Figure 2). A negative, weaker, but still significant, correlation between R<sub>ME</sub> and the light argon isotope concentration was also revealed (Figure 3). As it turned out, the latter was related in varying degrees with the concentration of hydrocarbon gases, with an increase in the molecular weight intensifying this bond. Thus, the calculated pairs of correlation coefficients of <sup>36</sup>Ar with pentanes (Figure 4), ethane and methane were 0.96, 0.59 and 0.45, respectively.



**Figure 2.** Correlations of the CH<sub>4</sub>/C<sub>2</sub>H<sub>6</sub> and <sup>3</sup>He/<sup>4</sup>He ratios. Samples: 1—eudialite complex; 2 and 3—differentiated complex, Series I + II and III–V, respectively; 4 and 5—endocontact and exocontact zones of the massif.

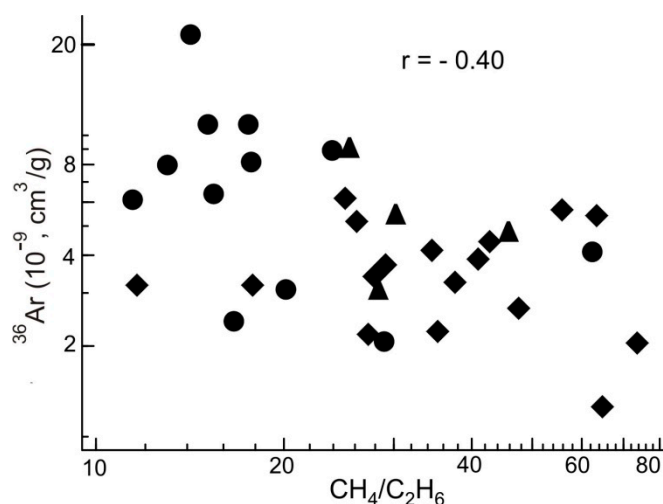


**Figure 3.** Relationships between the  $\text{CH}_4/\text{C}_2\text{H}_6$  ratios and  $^{36}\text{Ar}$  concentrations. The symbols are as in Figure 2.

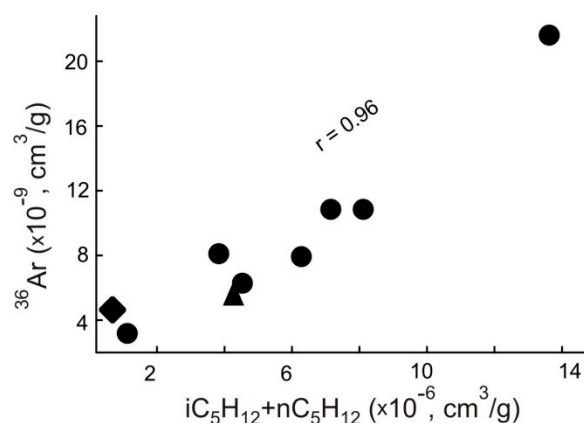


**Figure 4.** Correlations of the amount of pentanes and the  $^{36}\text{Ar}$  concentrations. The symbols are as in Figure 2.

Figures 2–4 show that the processes causing the fraction of its deep constituent in the fluid phase to decrease and the concentration of heavier hydrocarbons and the proportion of the atmogenic component to increase, largely coincided in both time and space. These observations are consistent with the previously established parallel increase in the proportion of a high molecular weight HCG and a decrease in the  $^3\text{He}/^4\text{He}$  ratio among the main Khibiny and Lovozero rock-forming minerals (aegirine–K–Na feldspar–nepheline) [76]. In the same sequence, the total average gas content of the minerals and the intensity of their post-magmatic transformations increased. Furthermore, a previous calculation [70] of the balance of helium and argon isotopes in the minerals of the Lovozero zeolitized juvite-urtite (feldspar urtite) from Series II of DC showed that zeolites, which make up about 20% of the sample volume, accounted for only 4% of the helium contained in the rock with a low  $^3\text{He}/^4\text{He}$  ratio, and 96% of the total  $^{36}\text{Ar}$  with a near atmospheric value of  $^{40}\text{Ar}/^{36}\text{Ar}$ . Therefore, in comparison with the associated nepheline, sodalite, feldspar and aegirine, the zeolites differed with the lowest  $\text{CH}_4/\text{C}_2\text{H}_6$ .

No relationship was found between the concentrations of  $\text{CH}_4$  and  $^3\text{He}$  (Figure 5), whereas in the case of methane from a predominantly mantle source, a positive correlation between these components could be expected. The same figure showed that the value of the  $\text{CH}_4/^3\text{He}$  ratio in the Lovozero rocks significantly exceeded the estimates of those in mantle gases ( $1 \times 10^5$ – $1 \times 10^7$ ) and mainly corresponded to the crustal values estimated at  $1 \times 10^{10}$ – $1 \times 10^{13}$  [31,33,37,77].

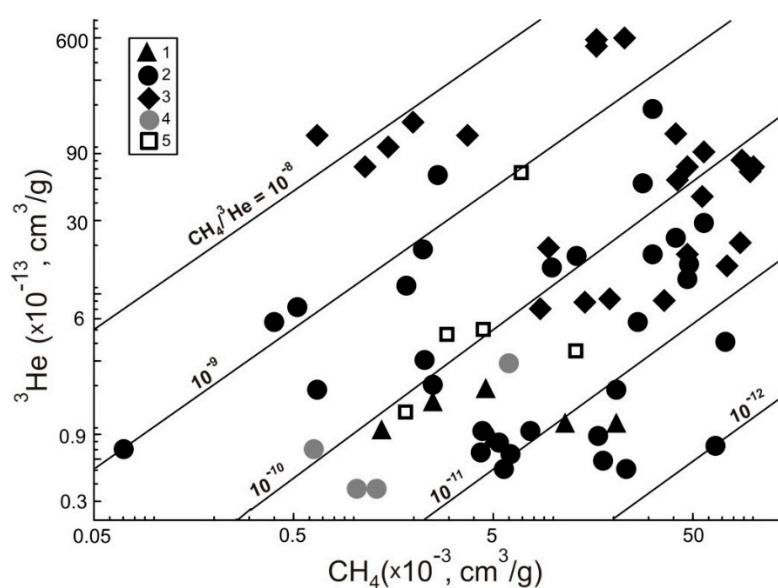


**Figure 5.** Relationship of the methane and  $^3\text{He}$  concentrations. Samples: 1—eudialite complex; 2 and 3—differentiated complex, Series I + II and III–V, respectively; 4 and 5—endocontact and exocontact zones of the massif. The inclined lines are equal ratios of  $\text{CH}_4/{}^3\text{He}$ .

More than 30 years ago, Marty and Jambon [29] showed the possibility that combining carbon-helium and isotope-helium systems could be the most important characteristic of deep fluids in mantle and subduction zones. Thus, a double diagram of the  ${}^3\text{He}/{}^4\text{He}$  ( $R/R_a$ ,  ${}^4\text{He}/{}^3\text{He}$ )– $\text{CH}_4/{}^3\text{He}$  type, in one form or another, is often used to determine the methane sources in the gases of different geological environments [30,33,35,38,39,41,45–47].

The figurative points of the Lovozero gas samples in such a diagram form a vast field that partially overlaps the region of the crustal values of the considered parameters and the adjacent part of the hypothetical mixture of the mantle and crust sources (Figure 6). The latter usually refers to gases of a thermogenic origin. However, the high (from  $1 \times 10^{11}$  to  $1 \times 10^{14}$ )  $\text{CH}_4/{}^3\text{He}$  ratios in the Sea of Japan’s oil and gas fields are considered to be the result of abiogenic methane formation by a  $\text{CO}_2$  reduction [28]. In the present case, about a quarter of the Lovozero samples (mainly the upper part of the DC, including the rocks of the endocontact massif) are characterized by “crustal” values. Of the remaining ones, more than half of the points are located below these areas. In general, the field of Lovozero gases is located at a considerable distance from gases with methane of a distinct or predominantly mantle origin, which include the gases of geothermal fluids from the East Pacific Rise  $13^\circ \text{N}$  and  $21^\circ \text{N}$  and the Mid-Atlantic Ridge [43], as well as micro-inclusion gases in the olivinites and pyroxenites of the Kovdor and Seblyavr massifs of the Kola alkaline province (data on the  ${}^3\text{He}/{}^4\text{He}$  ratios have been borrowed from Reference [72]).

The intermediate position between the mantle region and the field of Lovozero samples is occupied by magmatic gases of the Zambales Ophiolite in the Philippines [78] and carbonatites from the Sallanlatwa and Sokli complexes of the Kola alkaline province (previously unpublished data collected by the author), abiogenic methane from the hot springs in China [37], as well as magmatic gases that partially enter the Lovozero field from the Xujiaweizi area of the Songliao Basin (China) [38] and abiogenic methane from the geothermal field of the Vicano–Cimino Volcanic District (Italy), which is formed due to the reduction of  $\text{CO}_2$  [44]. In the latter cases, even if the samples included in the diagram fell into the mixing zone of the crust and mantle end members or, for example, in the Xujiaweizi area of the Songliao Basin, China, a strong correlation between  $\text{CH}_4/{}^3\text{He}$  and  ${}^3\text{He}/{}^4\text{He}$  was found [38], in the aggregate of the different criteria the methane was not a mixture of thermogenic (or bacterial) and mantle. It can be assumed that only the latter’s presence in one proportion or another, or the possibility of a mantle source of carbon, was involved in the formation of methane.

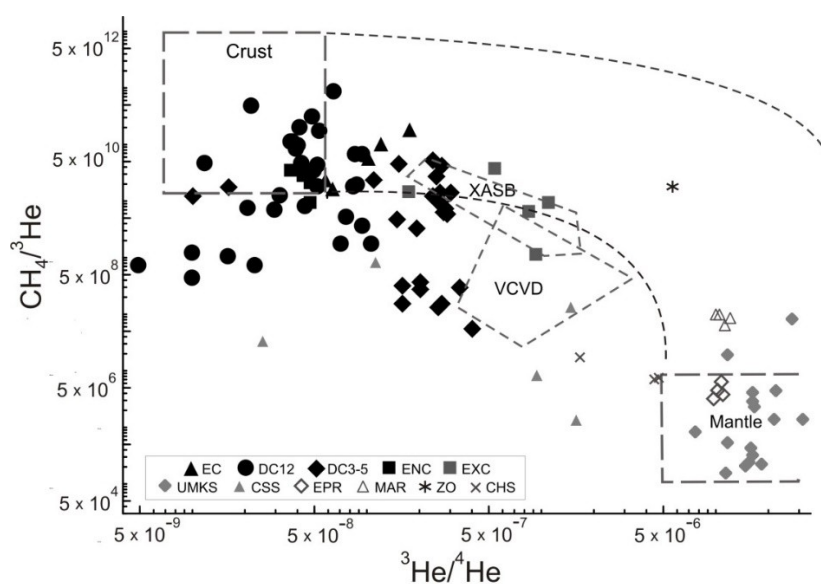


**Figure 6.** Plot of the  $\text{CH}_4/{}^3\text{He}$  vs.  ${}^3\text{He}/{}^4\text{He}$  of abiogenic gases from the Lovozero massif and some other geological settings. The Lovozero samples are from: EC—eudialite complex, DC12 and DC3–5—differentiated complex (Series I and II and III–V, respectively), ENC and EXC—endocontact and exocontact of the massif, respectively. UMKS—ultramafites from the Kovdor and Sebyavr complexes of the Kola Alkaline Province ([72] and the unpublished author’s data), CSS—carbonatites from the Sallanlatva and Sokli complexes of the Kola Alkaline Province (unpublished author’s data), EPR—the East Pacific Rise  $13^\circ\text{N}$  and  $21^\circ\text{N}$  [43], MAR—the Mid-Atlantic Ridge (ibid), ZO—the Zambales Ophiolite in the Philippines [78] and CHS—hot springs in China [37]. The dashed lines show the crust and mantle fields [31,33,34,37,45,46,77,79]; VCVD—the Vicano–Cimino Volcanic District, Italy [44], and XASB—the Xujiaweizi area of the Songliao Basin, China [38].

The presence of, albeit a weak, negative correlation among the  $\text{CH}_4/{}^3\text{He}$  and  ${}^3\text{He}/{}^4\text{He}$  ratios in the entire set of Lovozero samples, and the location of some of them in the diagram, also allows for the presence of a very insignificant fraction of mantle methane in the rocks of the lower DC series, and especially in the exocontact of the massif. It is this source, at least primarily magmatic, that can be determined for  $\text{CH}_4$  in the apgaitic and miaskitic rocks of the Ilimaussaq and Khibiny massifs, based on an analysis of the mineral equilibria [11–13] and the isotopic compositions of carbon and hydrogen of the HCG [25,67]. The authors believe that methane could be the predominant carbon component of the fluid during the magmatic crystallization of such rocks. However, the observed ratios of methane and helium isotopes in the Lovozero rocks can only be due to mantle-derived carbon, which later becomes part of the  $\text{CH}_4$ . Estimates of the crystallization process’ redox and temperature conditions showed that the carbon was in the form of  $\text{CO}_2$  in equilibrium with the melt fluid [80]. According to the thermodynamic calculations of Ryabchikov and Kogarko [19,20], under the redox conditions characteristic of the Khibiny massif, at high temperatures, carbon should also be in the form of  $\text{CO}_2$  in the fluid and carbonate anions during the melt. According to these calculations, the presence of  $\text{CH}_4$  in the fluid phase can be allowed only in small quantities.

However, the previously established [70] increasing concentrations of  $\text{CH}_4$  and  ${}^3\text{He}$ , and the ratios of  ${}^3\text{He}/{}^4\text{He}$  and  $\text{CH}_4/\text{C}_2\text{H}_6$  in the fenites and fenitized gneisses of the exocontact of the Lovozero massif, as compared with the rocks of the endocontact (Figure 7), may indicate the appearance of a significant amount of methane in the fluid even during the magmatic stage in the formation of the massif. The rocks of the endocontact are represented by uneven coarse-grained and pegmatoid massive nepheline syenites (up to microclinites), which are typical for this situation. Changes in the mineral composition of the Archean orthogneisses also corresponded to those described earlier, for example in References [81,82].

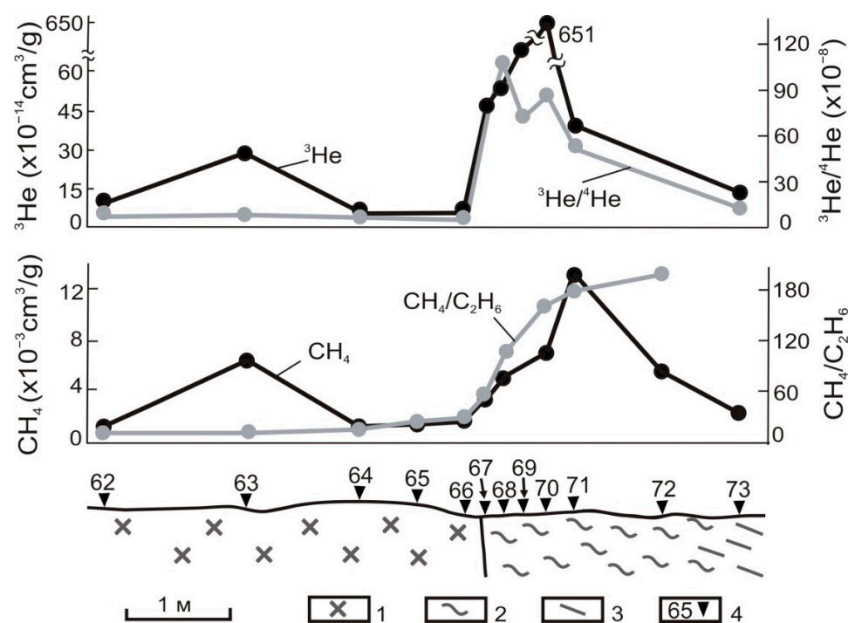


**Figure 7.** Distribution of the  $^3\text{He}$  and  $\text{CH}_4$  concentrations and  $^3\text{He}/^4\text{He}$  and  $\text{CH}_4/\text{C}_2\text{H}_6$  ratios in the contact zone of the Lovozero massif. Symbols: 1—nepheline syenites of the endocontact; 2—fenites and fenitized gneisses; 3—unaltered gneisses; 4—sampling localities. From Reference [70], with minor modifications.

It can be assumed that a fenitization halo around the nepheline-syenite massifs was formed mainly during the late magmatic stage of their evolution, under the influence of several pulses of alkaline heterophase fluid, whose generation took place in the relatively narrow (up to 200 m) endocontact zone [83,84]. The separation of the fluid phase led to a change in the mineral and chemical composition of the rocks in this zone, which are very different from the nepheline syenites in the massif's interior. Judging by the peculiar properties of the distribution of  $\text{CH}_4$  and  $^3\text{He}$  in the exocontact, the ratios of these components in different portions of the acting fluid was not the same. The formation temperatures of such fenitization halos are estimated to be 500–800 °C [84,85]. The maximum value in this zone of  $^3\text{He}/^4\text{He} = 111 \times 10^{-8}$  in the fenite 15 cm from the contact nearly coincides with the highest value found in the massif's intrusive rocks. It is close to the upper estimate of the initial ratio in the trapped helium [70].

Thus, along with: (a) the features of the distribution of HCG in the rocks and minerals [4,14,22,66], (b) variations in the isotopic compositions of carbon and hydrogen [21,25,86] as well as noble gases [70], (c) the molecular mass distribution of gaseous alkanes [9,18,22,23] and (d) the data thermodynamic calculations [20,21], thermobarometry and Raman spectroscopy of the fluid microinclusions [64,65,87], the peculiarities of the relationship between the Lovozero hydrocarbon and the isotopes of noble gases could also indicate that the abiogenic generation HCG and their transformations occurred at different stages of the mineral formation.

In the magmatic stage, methane could appear in the fluid, particularly during the crystallization of aegirine and alkaline amphibole [13]. The interaction of water and previously formed graphite [20] is another probable way of generating hydrocarbon gases. As the temperature decreased under favorable conditions, reactions of the Fischer–Tropsch-type (RTFT)— $(n\text{CO}_2 + (3n + 1)\text{H}_2 = \text{C}_n\text{H}_{2n} + 2 + 2n\text{H}_2\text{O})$  could have started. The iron-containing phases, aluminosilicates and especially the zeolites [88–90] and microporous aqueous titan-, niobo- and zircon- osilicates, to which accumulations of bituminous substances are constantly confined in these massifs [91], could also be the catalysts and promoters of such reactions that can self-sustain due to the heat generation. The initial RTFT, along with the magmatic  $\text{CO}_2$  and hydrogen, being a product of the evolution of the magmatic fluid, was probably also generated by the interaction of iron-containing minerals and aluminosilicates with water, which

occurs during the formation of aegirine, magnetite, cancrinite and zeolites [7,64,65]. Together with other data, the results of this work show that the RTFT synthesis could be part of a complex multistage process of hydrocarbon formation, which included oxidation and dehydrogenation, polymerization and condensation reactions, and occurred during the further evolution of the system [88,92,93], when the magmatic was diluted fluid with circulating paleometeor waters.

## 5. Conclusions

Despite the long history of research, the origin of the hydrocarbon gases naturally occurring in some nepheline-syenite massifs in concentrations that are unusually high for magmatic complexes remains a subject of discussion. One of the approaches to understanding the nature of these gases in the Lovozero massif rocks involves coupling their distribution with the abundances of helium and argon isotopes, which are recognized as geochemical tracers. In our study, extraction of the gas components contained in fluid micro-inclusions was carried out by a mechanical grinding of rock and mineral samples.

Along with wide (mainly up to three orders of magnitude) variations in the characteristics of the gases in general, a positive correlation was found for such important indicators as  $^3\text{He}/^4\text{He}$  and  $\text{CH}_4/\text{C}_2\text{H}_6$ . In contrast, a negative correlation of the latter with the concentration of  $^{36}\text{Ar}$  was revealed. The distribution of  $^{36}\text{Ar}$  was also directly, to varying degrees, associated with the distribution of HCG, with this bond being strengthened along with increasing molecular weight. It turned out that the processes of increasing the share of heavier hydrocarbons in the composition of the gases, the loss of the deep component and the addition of the atmogenic one to the fluid phase, largely coincided in both time and space. In the absence of any correlation between  $\text{CH}_4$  and  $^3\text{He}$ , the value of the ratio of  $\text{CH}_4/{}^3\text{He}$  in the Lovozero gases substantially exceeded the estimates of the ratio in the gases of a mantle origin and mainly corresponded to the crustal values. Nevertheless, the observed ratios of methane and helium isotopes allowed for the presence of an insignificant fraction of mantle  $\text{CH}_4$ , or at least the initial carbon, in the rocks of the lower series of DC and in the exocontact of the massif.

Together with other data, the peculiarities of the relationship between the Lovozero hydrocarbon and the isotopes of noble gases could indicate extended abiogenic generation and transformation of the HCG at different stages of the magmatic and post-magmatic mineral formation.

It seems that a more detailed study of the relationship between the distribution of HCG,  $\text{H}_2$  and noble gas (Ne, Ar and Ne) isotopes in the Lovozero and other nepheline-syenite massifs will significantly advance the long-standing problem of the origin of reduced gases in alkaline magmatic systems. Such studies should preferably be combined with the C and H isotopy and thermobarometry of fluid micro-inclusions.

**Funding:** This paper was prepared in the framework of State contract No 0226-2019-0051 of GI KSC RAS.

**Acknowledgments:** The author is very grateful to I. L. Kamensky for the methodological guidance and direct measurements of noble gas isotopes, S. V. Ikorsky for the methodological and technical support of gas chromatographic analyses, A. A. Avedisyan for performing part of the latter, and to the anonymous reviewer for valuable suggestions and comments.

**Conflicts of Interest:** The author declares no conflict of interest.

## References

1. Petersilie, I.A. *Geology and Geochemistry of Natural Gases and Disperse Bitumens of Some Geological Formations of the Kola Peninsula*; Nauka: Moscow, Russia, 1964. (In Russian)
2. Petersilie, I.A.; Sørensen, H. Hydrocarbon gases and bituminous substances in rocks from the Ilímaussaq alkaline intrusion, South Greenland. *Lithos* **1970**, *3*, 59–76. [[CrossRef](#)]
3. Konnerup-Madsen, J.; Larsen, E.; Rose-Hansen, J. Hydrocarbon-rich fluid inclusions in minerals from the alkaline Ilímaussaq intrusion. *South Greenl. Bull. Minéral.* **1979**, *102*, 642–653. [[CrossRef](#)]
4. Ikorsky, S.V.; Nivin, V.A.; Pripachkin, V.A. *Gas Geochemistry of Endogenic Formations*; Nauka: St.-Petersburg, Russia, 1992. (In Russian)

5. Konnerup-Madsen, J. A review of the composition and evolution of hydrocarbon gases during solidification of the Ilímaussaq alkaline complex. *South Greenl. Geol. Greenl. Surv. Bull.* **2001**, *190*, 159–166. [[CrossRef](#)]
6. Nivin, V.A. Occurrence forms, composition, distribution, origin and potential hazard of natural hydrogen–hydrocarbon gases in ore deposits of the Khibiny and Lovozero massifs: A review. *Minerals* **2019**, *9*, 535. [[CrossRef](#)]
7. Nivin, V.A.; Treloar, P.J.; Konopleva, N.G.; Ikorsky, S.V. A review of the occurrence, form and origin of C-bearing species in the Khibiny alkaline igneous complex, Kola Peninsula, NW Russia. *Lithos* **2005**, *85*, 93–112. [[CrossRef](#)]
8. Nivin, V.A. Diffusely disseminated hydrogen–hydrocarbon gases in rocks of nepheline syenite complexes. *Geochem. Int.* **2009**, *47*, 672–691. [[CrossRef](#)]
9. Nivin, V.A. Free hydrogen-hydrocarbon gases from the Lovozero loparite deposit (Kola Peninsula, NW Russia). *Appl. Geochem.* **2016**, *74*, 44–55. [[CrossRef](#)]
10. Salvi, S.; Williams-Jones, A.E. Alteration, HFSE mineralisation and hydrocarbon formation in peralkaline igneous systems: Insights from the Strange Lake Pluton, Canada. *Lithos* **2006**, *91*, 19–34. [[CrossRef](#)]
11. Krumrei, T.V.; Pernicka, E.; Kaliwoda, M.; Markl, G. Volatiles in a peralkaline system: Abiogenic hydrocarbons and F–Cl–Br systematics in the naujaite of the Ilímaussaq intrusion, South Greenland. *Lithos* **2007**, *95*, 298–314. [[CrossRef](#)]
12. Graser, G.; Potter, J.; Kohler, J.; Markl, G. Isotope, major, minor and trace element geochemistry of late-magmatic fluids in the peralkaline Ilímaussaq intrusion, South Greenland. *Lithos* **2008**, *106*, 207–221. [[CrossRef](#)]
13. Markl, G.; Marks, M.A.W.; Frost, B.R. On the controls of oxygen fugacity in the generation and crystallization of peralkaline melts. *J. Petrol.* **2010**, *51*, 1831–1847. [[CrossRef](#)]
14. Nivin, V.A. Variations in the composition and origin of hydrocarbon gases from inclusions in minerals of the Khibiny and Lovozero plutons, Kola Peninsula, Russia. *Geol. Ore Deposit.* **2011**, *53*, 699–707. [[CrossRef](#)]
15. Nivin, V.A. Gas Components in Magmatic Rocks: Geochemical, Mineragenic and Environmental Aspects and Results. Ph.D. Thesis, Vernadsky Institute of Geochemistry and Analytical Chemistry of Russian Academy of Sciences, Moscow, Russia, 2013; p. 354. (In Russian).
16. Vasyukova, O.V.; Williams-Jones, A.E.; Blamey, N.J.F. Fluid evolution in the Strange Lake granitic pluton, Canada: Implications for HFSE mobilisation. *Chem. Geol.* **2016**, *444*, 83–100. [[CrossRef](#)]
17. Marks, M.A.W.; Markl, G. A global review on agpaitic rocks. *Earth Sci. Rev.* **2017**, *173*, 229–258. [[CrossRef](#)]
18. Beeskow, B.; Treloar, P.J.; Rankin, A.H.; Vennemann, T.W.; Spangenberg, J. A reassessment of models for hydrocarbon generation in the Khibiny nepheline syenite complex, Kola Peninsula, Russia. *Lithos* **2006**, *91*, 1–18. [[CrossRef](#)]
19. Ryabchikov, I.D.; Kogarko, L.N. Magnetite compositions and oxygen fugacities of the Khibina magmatic system. *Lithos* **2006**, *91*, 35–45. [[CrossRef](#)]
20. Ryabchikov, I.D.; Kogarko, L.N. Redox potential of the Khibiny magmatic system and genesis of abiogenic hydrocarbons in alkaline plutons. *Geol. Ore Deposit.* **2009**, *51*, 425–440. [[CrossRef](#)]
21. Potter, J.; Longstaffe, F.J. A gas-chromatograph, continuous flow-isotope ratio mass-spectrometry method for  $\delta^{13}\text{C}$  and  $\delta\text{D}$  measurement of complex fluid inclusion volatiles: Examples from the Khibina alkaline igneous complex, northwest Russia and the south Wales coalfields. *Chem. Geol.* **2007**, *244*, 186–201. [[CrossRef](#)]
22. Nivin, V.A. Molecular-mass distribution of gas hydrocarbons and the problem of their origin in alkaline magmatic complexes. In *Alkaline Magmatism, Its Sources and Plums*; Vladykin, N.V., Ed.; Publishing House of the Institute of Geography SB RAS: Irkutsk, Russia, 2008; pp. 107–130. (In Russian)
23. Nivin, V.A. Molecular–mass distribution of saturated hydrocarbons in gas of the Lovozerskii nepheline–syenite massif. *Dokl. Earth Sci.* **2009**, *429*, 1580–1582. [[CrossRef](#)]
24. Laier, T.; Nytoft, H.P. Bitumen biomarkers in the Mid-Proterozoic Ilímaussaq intrusion, Southwest Greenland—A challenge to the mantle gas theory. *Mar. Petrol. Geol.* **2012**, *30*, 50–65. [[CrossRef](#)]
25. Potter, J.; Salvi, S.; Longstaffe, F. Abiogenic hydrocarbon isotopic signatures in granitic rocks: Identifying pathways of formation. *Lithos* **2013**, *182–183*, 114–124. [[CrossRef](#)]
26. Etiope, G.; Sherwood Lollar, B. Abiotic methane on Earth. *Rev. Geophys.* **2013**, *51*, 276–299. [[CrossRef](#)]
27. Sephton, M.A.; Hazen, R.M. On the Origins of Deep Hydrocarbons. *Rev. Miner. Geochem.* **2013**, *75*, 449–465. [[CrossRef](#)]

28. Wakita, H.; Sano, Y.  $^3\text{He}/^4\text{He}$  ratios in  $\text{CH}_4$ -rich natural gases suggest magmatic origin. *Nature* **1983**, *305*, 792–794. [[CrossRef](#)]
29. Marty, B.; Jambon, A.  $\text{C}/^3\text{He}$  in volatile fluxes from the solid Earth: Implications for carbon geodynamics. *Earth Planet. Sci. Lett.* **1987**, *83*, 16–26. [[CrossRef](#)]
30. Poreda, R.J.; Jeffrey, A.W.A.; Kaplan, I.R.; Craig, H. Magmatic helium in subduction zone natural gases. *Chem. Geol.* **1988**, *71*, 199–210. [[CrossRef](#)]
31. Jean-Baptiste, P.; Charlou, J.L.; Stievenard, M.; Donval, J.P.; Bougault, H.; Mevel, C. Helium and methane measurements in hydrothermal fluids from the Mid Atlantic Ridge: The Snake Pit site at  $23^\circ$  N. *Earth Planet. Sci. Lett.* **1991**, *106*, 17–28. [[CrossRef](#)]
32. Jean-Baptiste, P.; Fourré, E.; Charlou, J.L.; German, C.; Radford-Knoery, J. Helium isotopes at the Rainbow hydrothermal site (Mid-Atlantic Ridge,  $36^\circ 14'$  N). *Earth Planet. Sci. Lett.* **2004**, *221*, 325–335. [[CrossRef](#)]
33. Jenden, P.D.; Hilton, D.R.; Kaplan, I.R.; Craig, H. Abiogenic hydrocarbons and Mantle helium in oil and gas fields. In *The Future of Energy Gases*; Howell, D.G., Ed.; US Geological Survey Professional Paper, 1570; US Government Print Office: Washington, DC, USA, 1993; pp. 31–56.
34. Tolstikhin, I.N.; Marty, B. The evolution of terrestrial volatiles: A view from helium, neon, argon and nitrogen isotope modelling. *Chem. Geol.* **1998**, *147*, 27–52. [[CrossRef](#)]
35. Pinti, D.L.; Marty, B. Noble gases in oil and gas fields: Origins and processes. In *Fluids and Basin Evolution*; Kyser, K., Ed.; Mineralogical Association of Canada: Québec, QC, Canada, 2000; pp. 160–196.
36. Ballentine, C.J.; Burgess, R.; Marty, B. Tracing fluid origin, transport and interaction in the crust. *Rev. Miner. Geochem.* **2002**, *47*, 539–614. [[CrossRef](#)]
37. Dai, J.; Yang, S.; Chen, H.; Shen, X. Geochemistry and occurrence of inorganic gas accumulations in Chinese sedimentary basins. *Org. Geochem.* **2005**, *36*, 1664–1688. [[CrossRef](#)]
38. Jin, Z.; Zhang, L.; Wang, Y.; Cui, Y.; Milla, K. Using carbon, hydrogen and helium isotopes to unravel the origin of hydrocarbons in the Xujiaweizi area of the Songliao Basin, China. *Episodes* **2009**, *32*, 167–176. [[CrossRef](#)] [[PubMed](#)]
39. Lavrushin, V.Y.; Polyak, B.G.; Pokrovskii, B.G.; Kopp, M.L.; Buachidze, G.I.; Kamenskii, I.L. Isotopic–geochemical peculiarities of gases in mud volcanoes of Eastern Georgia. *Lithol. Miner. Resour.* **2009**, *44*, 183–197. [[CrossRef](#)]
40. Sherwood Lollar, B.; Ballentine, C. Insights into deep carbon derived from noble gases. *Nat. Geosci.* **2009**, *2*, 543–547. [[CrossRef](#)]
41. Kikvadze, O.; Lavrushin, V.; Pokrovsky, B.; Polyak, B. Gases from mud volcanoes of western and central Caucasus. *Geofluids* **2010**, *10*, 486–496. [[CrossRef](#)]
42. Holland, G.; Sherwood Lollar, B.; Li, L.; Lacrampe-Couloume, G.; Slater, G.F.; Ballentine, C.J. Deep fracture fluids isolated in the crust since the Precambrian era. *Nature* **2013**, *497*, 357–360. [[CrossRef](#)]
43. Sano, Y.; Fischer, T.P. The analysis and Interpretation of Noble Gases in Modern Hydrothermal Systems. In *The Noble Gases as Geochemical Tracers. Advances in Isotope Geochemistry*; Burnard, P., Hoefs, J., Eds.; Springer: Berlin/Heidelberg, Germany, 2013; pp. 249–317.
44. Cinti, D.; Tassi, F.; Procesi, M.; Bonini, M.; Capecchiacci, F.; Voltattorni, N.; Vaselli, O.; Quattrocchi, F. Fluid geochemistry and geothermometry in the unexploited geothermal field of the Vicano–Cimino Volcanic District (Central Italy). *Chem. Geol.* **2014**, *371*, 96–114. [[CrossRef](#)]
45. Ni, Y.; Dai, J.; Tao, S.; Wu, X.; Liao, F.; Wu, W.; Zhang, D. Helium signatures of gases from the Sichuan Basin, China. *Org. Geochem.* **2014**, *74*, 33–43. [[CrossRef](#)]
46. Liu, Q.; Dai, J.; Jin, Z.; Li, J.; Wu, X.; Meng, Q.; Yang, C.; Zhou, Q.; Feng, Z.; Zhu, D. Abnormal carbon and hydrogen isotopes of alkane gases from the Qingshen gas field. *J. Asian Earth Sci.* **2016**, *115*, 285–297. [[CrossRef](#)]
47. Tolstikhin, I.N.; Ballentine, C.J.; Polyak, B.G.; Prasolov, E.M.; Kikvadze, O.E. The noble gas isotope record of hydrocarbon field formation time scales. *Chem. Geol.* **2017**, *471*, 141–152. [[CrossRef](#)]
48. Prinzhofer, A.; Cisse, C.S.T.; Diallo, A.B. Discovery of a large accumulation of natural hydrogen in Bourakebougou (Mali). *Int. J. Hydrogen Energy* **2018**, *43*, 19315–19326. [[CrossRef](#)]
49. Warr, O.; Giunta, T.; Ballentine, C.J.; Sherwood Lollar, B. Mechanisms and rates of  $^4\text{He}$ ,  $^{40}\text{Ar}$ , and  $\text{H}_2$  production and accumulation in fracture fluids in Precambrian Shield environments. *Chem. Geol.* **2019**, *530*, 119322. [[CrossRef](#)]

50. Byrne, D.J.; Barry, P.H.; Lawson, M.; Ballentine, C.J. The use of noble gas isotopes to constrain subsurface fluid flow and hydrocarbon migration in the East Texas Basin. *Geochim. Cosmochim. Acta* **2020**, *268*, 186–208. [[CrossRef](#)]
51. Vlasov, K.A.; Kuz'menko, M.Z.; Es'kova, E.M. *The Lovozero Alkali Massif*; Fry, D.G.; Syers, K., Translators; Oliver & Boyd: Edinburgh, UK, 1966.
52. Gerasimovsky, V.I.; Volkov, V.P.; Kogarko, L.N.; Polyakov, A.I.; Saprykina, T.V.; Balashov, Y.A. *The Geochemistry of the Lovozero Alkaline Massif*; Part 1 and Part 2; Australian National University Press: Canberra, Australia, 1966.
53. Bussen, I.V.; Sakharov, A.S. *Petrology of the Lovozero Alkaline Massif*; Nauka: Leningrad, Russia, 1972. (In Russian)
54. Pekov, I.V. *Lovozero Massif: History, Pegmatites, Minerals*; Ocean Pictures Ltd.: Moscow, Russia, 2000.
55. Arzamastsev, A.A.; Arzamastseva, L.V.; Zhirova, A.M.; Glaznev, V.N. Model of formation of the Khibiny–Lovozero ore-bearing volcanic–plutonic complex. *Geol. Ore Deposit.* **2013**, *55*, 341–356. [[CrossRef](#)]
56. Suk, N.I.; Kotel'nikov, A.R.; Viryus, A.A. Crystallization of loparite in alkaline fluid-magmatic systems (from experimental and mineralogical data). *Russ. Geol. Geophys.* **2013**, *54*, 436–453. [[CrossRef](#)]
57. Pakhomovsky, Y.A.; Ivanyuk, G.Y.; Yakovenchuk, V.N. Loparite-(Ce) in rocks of the Lovozero layered complex at Mt. Karnasurt and Mt. Kedykvyrpakhk. *Geol. Ore Deposit.* **2014**, *56*, 685–698. [[CrossRef](#)]
58. Ivanyuk, G.Y.; Pakhomovsky, Y.A.; Yakovenchuk, V.N. Eudialyte-group minerals in rocks of Lovozero layered complex at Mt. Karnasurt and Mt. Kedykvyrpakhk. *Geol. Ore Deposit.* **2015**, *57*, 600–613. [[CrossRef](#)]
59. Kalashnikov, A.O.; Konopleva, N.G.; Pakhomovsky, Y.A.; Ivanyuk, G.Y. Rare earth deposits of the Murmansk Region, Russia—A review. *Econ. Geol.* **2016**, *111*, 1529–1559. [[CrossRef](#)]
60. Kogarko, L.N. Geochemistry of fractionation of coherent elements (Zr and Hf) during the profound differentiation of peralkaline magmatic systems: A case study of the Lovozero complex. *Geochem. Int.* **2016**, *54*, 1–6. [[CrossRef](#)]
61. Krivovichev, V.G.; Charykova, M.V. Mineral systems, their types, and distribution in nature. I. Khibiny, Lovozero, and the Mont Saint-Hilaire. *Geol. Ore Dep.* **2016**, *58*, 551–558. [[CrossRef](#)]
62. Zartman, R.E.; Kogarko, L.N. Lead isotopic evidence for interaction between plume and lower crust during emplacement of peralkaline Lovozero rocks and related rare-metal deposits, East Fennoscandia, Kola Peninsula, Russia. *Contrib. Mineral. Petrol.* **2017**, *172*, 32. [[CrossRef](#)]
63. Mikhailova, J.A.; Ivanyuk, G.Y.; Kalashnikov, A.O.; Pakhomovsky, Y.A.; Bazai, A.V.; Yakovenchuk, V.N. Petrogenesis of the Eudialyte Complex of the Lovozero Alkaline Massif (Kola Peninsula, Russia). *Minerals* **2019**, *9*, 581. [[CrossRef](#)]
64. Potter, J.; Rankin, A.H.; Treloar, P.J.; Nivin, V.A.; Ting, W.; Ni, P. A preliminary study of methane inclusions in alkaline igneous rocks of the Kola igneous province, Russia: Implications for the origin of methane in igneous rocks. *Eur. J. Miner.* **1998**, *10*, 1167–1180. [[CrossRef](#)]
65. Potter, J.; Rankin, A.H.; Treloar, P.J. Abiogenic Fischer-Tropsch synthesis of hydrocarbons in alkaline igneous rocks; fluid inclusion, textural and isotopic evidence from the Lovozero complex, NW Russia. *Lithos* **2004**, *75*, 311–330. [[CrossRef](#)]
66. Nivin, V.A. Gas concentrations in minerals with reference to the problem of the genesis of hydrocarbon gases in rocks of the Khibiny and Lovozero massifs. *Geochem. Int.* **2002**, *40*, 883–898.
67. Potter, J.; Konnerup-Madsen, J. A review of the occurrence and origin of abiogenic hydrocarbons in igneous rocks. In *Hydrocarbons in Crystalline Rocks*; Petford, N., McCaffrey, K.J.W., Eds.; The Geological Society of London: London, UK, 2003; pp. 151–173.
68. Nivin, V.A.; Kamensky, I.L.; Tolstikhin, I.N. Helium and argon isotope abundances in rocks of Lovozero alkaline massif. *Isotopenpraxis* **1993**, *28*, 281–287. [[CrossRef](#)]
69. Nivin, V.A.; Ikorsky, S.V. Some genetic features of the Lovozero rare-metal deposits (NW Russia) as it follows from noble gas (He, Ar) isotope abundances. In *Deep-Seated Magmatism, Magmatic Sources and the Problem of Plumes*; Dalnauka: Vladivostok, Russia, 2002; pp. 230–253.
70. Nivin, V.A. Helium and argon isotopes in rocks and minerals of the Lovozero alkaline massif. *Geochem. Int.* **2008**, *46*, 482–502. [[CrossRef](#)]
71. Marty, B.; Tolstikhin, I.N.; Kamensky, I.L.; Nivin, V.A.; Balaganskaya, E.G.; Zimmermann, J.-L. Plume-derived rare gases in 380 Ma carbonatites from the Kola region (Russian) and the argon isotopic composition in the deep mantle. *Earth Planet. Sci. Lett.* **1998**, *164*, 179–192. [[CrossRef](#)]

72. Tolstikhin, I.N.; Kamensky, I.L.; Marty, B.; Nivin, V.A.; Vetrin, V.R.; Balaganskaya, E.G.; Ikorsky, S.V.; Gannibal, M.A.; Weiss, D.; Verhulst, A.; et al. Rare gas isotopes and parent trace elements in ultrabasic-alkaline-carbonatite complexes, Kola Peninsula: Identification of lower mantle plume component. *Geochim. Cosmochim. Acta* **2002**, *66*, 881–901. [CrossRef]
73. Kramm, U.; Kogarko, L.N. Nd and Sr isotope signatures of the Khibina and Lovozero agpaite centres, Kola Alkaline Province, Russia. *Lithos* **1994**, *32*, 225–242. [CrossRef]
74. Arzamastsev, A.A.; Bea, F.; Glaznev, V.N.; Arzamastseva, L.V.; Montero, P. Kola Alkaline Province in the Paleozoic: Evaluation of Primary Mantle Magma Composition and Magma Generation Conditions. *Russ. J. Earth Sci.* **2001**, *3*, 1–32. Available online: <http://rjes.agu.org/v03/tje01054/tje01054.htm> (accessed on 1 August 2020). [CrossRef]
75. Kogarko, L.N.; Lahaye, Y.; Brey, G.P. Plume-related mantle source of super-large rare metal deposits from the Lovozero and Khibina massifs on the Kola Peninsula, Eastern part of Baltic shield: Sr, Nd and Hf isotope systematics. *Miner. Petrol.* **2010**, *98*, 197–208. [CrossRef]
76. Nivin, V.A.; Ikorsky, S.V.; Avedisyan, A.A. Hydrocarbon and noble gases of fluid inclusions in minerals of alkaline and carbonatite complexes of the Kola province. In Proceedings of the Transactions of the XI International Conference on Thermobarogeochemistry, 8–12 September 2003; VNIISIMS: Alexandrov, Russia; pp. 277–292. (In Russian).
77. Welhan, J.A. Origins of methane in hydrothermal systems. *Chem. Geol.* **1988**, *71*, 183–198. [CrossRef]
78. Abrajano, T.A.; Sturchio, N.C.; Bohlke, J.K.; Lyon, G.L.; Poreda, R.J.; Stevens, C.M. Methane-hydrogen gas seeps, Zambales ophiolite, Philippines: Deep or shallow origin? *Chem. Geol.* **1988**, *71*, 211–222. [CrossRef]
79. Xu, S.; Nakai, S.; Wakita, H.; Wang, X. Mantle-derived noble gases from Songliao Basin, China. *Geochim. Cosmochim. Acta* **1995**, *59*, 4675–4683. [CrossRef]
80. Kogarko, L.N.; Kosztolanyi, C.; Ryabchikov, I.D. Geochemistry of the reduced fluid in alkali magmas. *Geochem. Int.* **1987**, *24*, 20–27.
81. Bardina, N.Y.; Popov, V.S. Fenites: Systematics, conditions of formation and significance for crustal magmatism. *Zap. Vseross. Mineral. O-va* **1994**, *123*, 1–19. (In Russian)
82. Arzamastsev, A.A.; Arzamastseva, L.V.; Zaraiskii, G.P. Contact interaction of agpaite magmas with basement gneisses: An example of the Khibina and Lovozero massifs. *Petrology* **2011**, *19*, 115–139. [CrossRef]
83. Kozlov, E.N.; Arzamastsev, A.A. Petrogenesis of metasomatic rocks in the fenitized zones of the Ozernaya Varaka alkaline ultrabasic complex, Kola Peninsula. *Petrology* **2015**, *23*, 45–67. [CrossRef]
84. Elliott, H.A.L.; Wall, F.; Chakhmouradian, A.R.; Siegfried, P.R.; Dahlgren, S.; Weatherley, S.; Finch, A.A.; Marks, M.A.W.; Dowman, E.; Deady, E. Fenites associated with carbonatite complexes: A review. *Ore Geol. Rev.* **2018**, *93*, 38–59. [CrossRef]
85. Sindern, S.; Kramm, U. Volume characteristics and element transfer of fenite aureoles: A case study from the Iivaara alkaline complex, Finland. *Lithos* **2000**, *51*, 75–93. [CrossRef]
86. Nivin, V.A.; Devirts, A.L.; Lagutina, Y.P. The origin of the gas phase in the Lovozero massif based on hydrogen-isotope data. *Geochem. Int.* **1995**, *32*, 65–71.
87. Mokrushina, O.D.; Mokrushin, A.V.; Telezhkin, A.A. Fluid and melt inclusions in nepheline from the loparite deposit of the Lovozero alkaline massif. In *Alkaline Magmatism, its Sources and Plumes; Materials of the XV International Workshop*; Vladykin, N.V., Ed.; Institute of Geochemistry SB RAS: Simferopol-Irkutsk, Russia, 2019; pp. 274–284. (In Russian)
88. Lapidus, A.L.; Loktev, S.M. Present-day catalytic syntheses of hydrocarbons from carbon dioxide and hydrogen. *Zh. Vses. Khim. O-va Im. D.I. Mendeleeva* **1986**, *31*, 527–532. (In Russian)
89. Ione, K.G.; Mysov, V.M.; Stepanov, V.G.; Parmon, V.N. New data on the possibility of catalytic abiogenic synthesis of hydrocarbons in the earth's crust. *Petrol. Chem.* **2001**, *41*, 159–165.
90. Sharapov, V.N.; Ione, K.G.; Mazurov, M.P.; Mysov, V.M.; Perepechko, Y.V. *Geocatalysis and Evolution of Mantle-Crust Magmatogenic Fluid Systems*; Acad. Izd. Academic Publishing House “Geo”: Novosibirsk, Russia, 2007. (In Russian)
91. Chukanov, N.V.; Pekov, I.V.; Sokolov, S.V.; Nekrasov, A.N.; Ermolaeva, V.N.; Naumova, I.S. On the problem of the formation and geochemical role of bituminous matter in pegmatites of the Khibiny and Lovozero alkaline massifs, Kola Peninsula, Russia. *Geochem. Int.* **2006**, *44*, 715–728. [CrossRef]

92. Sherwood Lollar, B.; Lacrampe-Couloume, G.; Voglesonger, K.; Onstott, T.C.; Pratt, L.M.; Slater, G.F. Isotopic signatures of CH<sub>4</sub> and higher hydrocarbon gases from Precambrian Shield sites: A model for abiogenic polymerization of hydrocarbons. *Geochim. Cosmochim. Acta* **2008**, *72*, 4778–4795. [[CrossRef](#)]
93. Sinev, M.Y.; Fattakhova, Z.T.; Lomonosov, V.I.; Gordienko, Y.A. Kinetics of oxidative coupling of methane: Bridging the gap between comprehension and description. *J. Nat. Gas Chem.* **2009**, *18*, 273–287. [[CrossRef](#)]



© 2020 by the author. Licensee MDPI, Basel, Switzerland. This article is an open access article distributed under the terms and conditions of the Creative Commons Attribution (CC BY) license (<http://creativecommons.org/licenses/by/4.0/>).